Stellar winds from B supergiant stars: Exploring the δ-slow hydrodynamic solution

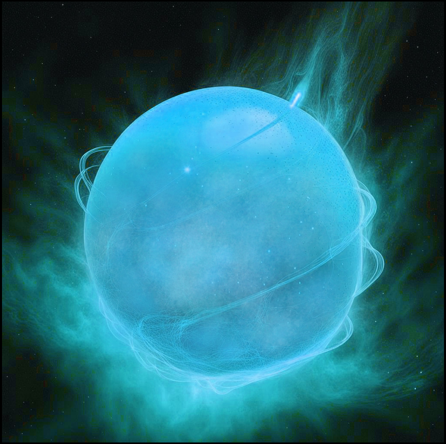

Roberto O. J. Venero

Institute of Astrophysics of La Plata (CONICET-UNLP)

Facultad de Ciencias Astronómicas y Geofísicas (FCAG)

La Plata National University (UNLP)

Argentina

Physics of Extreme Massive Stars
Marie-Curie-RISE project funded by the European Union

Stellar winds from B supergiant stars: Exploring the δ-slow hydrodynamic solution

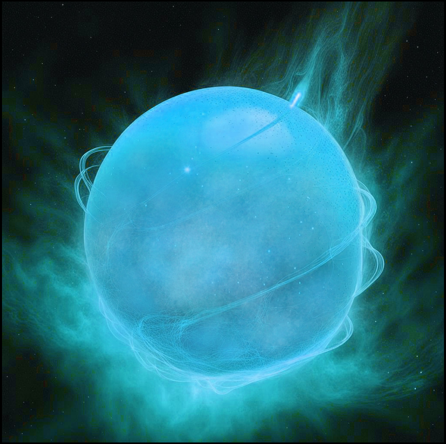

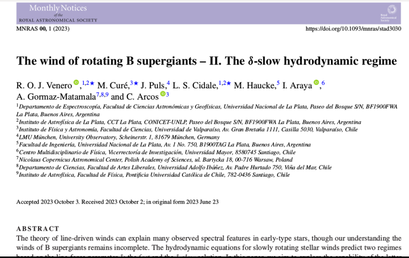

Monthly Notices of the Royal Astronomical Society
MNRAS **00**, 1 (2023) https://doi.org/10.1093/mnras/stad3030

The wind of rotating B supergiants – II. The δ-slow hydrodynamic regime

R. O. J. Venero,[1,2★] M. Curé,[3★] J. Puls,[4] L. S. Cidale,[1,2★] M. Haucke,[5] I. Araya,[6] A. Gormaz-Matamala[7,8,9] and C. Arcos[3]

[1] *Departamento de Espectroscopía, Facultad de Ciencias Astronómicas y Geofísicas, Universidad Nacional de La Plata, Paseo del Bosque S/N, BF1900FWA La Plata, Buenos Aires, Argentina*
[2] *Instituto de Astrofísica de La Plata, CCT La Plata, CONICET-UNLP, Paseo del Bosque S/N, BF1900FWA La Plata, Buenos Aires, Argentina*
[3] *Instituto de Física y Astronomía, Facultad de Ciencias, Universidad de Valparaíso, Av. Gran Bretaña 1111, Casilla 5030, Valparaíso, Chile*
[4] *LMU München, University Observatory, Scheinerstr. 1, 81679 München, Germany*
[5] *Facultad de Ingeniería, Universidad Nacional de La Plata, Av. 1 No. 750, B1900TAG La Plata, Buenos Aires, Argentina*
[6] *Centro Multidisciplinario de Física, Vicerrectoría de Investigación, Universidad Mayor, 8580745 Santiago, Chile*
[7] *Nicolaus Copernicus Astronomical Center, Polish Academy of Sciences, ul. Bartycka 18, 00-716 Warsaw, Poland*
[8] *Departamento de Ciencias, Facultad de Artes Liberales, Universidad Adolfo Ibáñez, Av. Padre Hurtado 750, Viña del Mar, Chile*
[9] *Instituto de Astrofísica, Facultad de Física, Pontificia Universidad Católica de Chile, 782-0436 Santiago, Chile*

Accepted 2023 October 3. Received 2023 October 2; in original form 2023 June 23

ABSTRACT
The theory of line-driven winds can explain many observed spectral features in early-type stars, though our understanding the winds of B supergiants remains incomplete. The hydrodynamic equations for slowly rotating stellar winds predict two regimes

Stellar winds

Flows of gas ejected from the surface of the star

It is a prominent phenomenon in OBA-type stars

Rigel (B8 Ia) and the Witch Head nebulae (*Star Shadows Remote Observatory*)

Stellar Winds: Why are they important?

Relevance of stellar winds

- Mass loss modifies the stellar evolution.
- Loss of angular momentum of stars.
- Estimation of distances and other relevant parameters.
- Interaction with the interstellar medium.
- Chemical evolution of galaxies.
- First generations of stars.
- Much more...
- **However, the stellar wind is intriguing in its own right.**

B-type supergiant stars

Main properties

- Heterogeneous group of stars.
- Diversity of evolutionary phases (blue region⇔red region of HR diagram).
- Photometric and spectroscopic variability.

Fundamental parameters

- $8\ M_\odot \lesssim$ Mass $\lesssim 50\ M_\odot$
- $10^{4,7}\ L_\odot \lesssim$ Luminosity $\lesssim 10^{5,6}\ L_\odot$
- $12\,000\ K \lesssim T_{\mathrm{eff}} \lesssim 25\,000\ K$
- $1.7 \lesssim \log g \lesssim 3$
- $20\ R_\odot \lesssim$ Radius $\lesssim 70\ R_\odot$
- $v \sin i \lesssim 100$ km s^{-1}

Region of the HR diagram occupied by B-type supergiant stars

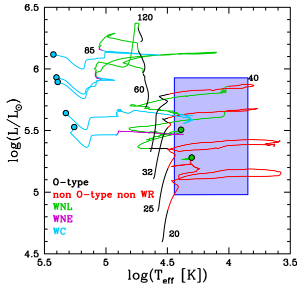

(Georgy+,2017)

B-type supergiant stars

Wind Parameters

- Mass-loss rates:
  $\dot{M} \sim 10^{-7}$ a 5×10^{-6} $M_{\odot}$ yr^{-1}
- Terminal velocities:
  $v_{\infty} \sim 200$ km s^{-1}(late) to 1 500 km s^{-1} (early)

$$\begin{cases} Q_{res} = \dfrac{\dot{M}}{R_{*} v_{\infty}^{2}} & \text{Resonance lines} \\ Q = \dfrac{\dot{M}}{(R_{*} v_{\infty})^{1,5}} & \text{Recombination lines (H}\alpha\text{)} \end{cases}$$

Optical depth invariant

Spectral variability

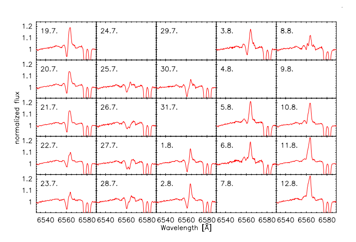

Hα line profiles of 55 Cygni (B3 Ia) from July to August 2013 (Haucke+,2016).

Radiation-driven wind theory

Brief historical overview

Milne (1924): Radiation force drives the ions, favored by the Doppler effect.

Lucy & Solomon (1970): Momentum transfer of the radiation field in resonance lines.

Castor, Abbott, & Klein (1975): CAK theory - The first analytical solution of radiation-driven winds (including weak line acceleration).

Abbott (1982): Line-force parameterization.

Basic hypotheses

- Stationary state.
- Homogeneous wind.
- Spherical symmetry.
- Point source (photons with radial direction).
- No rotation, magnetic fields, etc.

Hydrodynamic equations for the wind

Continuity equation

$$\dot{M} = -\frac{dM_*}{dt} = 4\pi r^2 \rho v = constant$$

Momentum equation

$$v\frac{\partial v}{\partial r} = -\frac{1}{\rho}\frac{\partial P}{\partial r} + g_r$$

$$g_r = -\frac{GM_*}{r^2} + g_{rad}^C + g_{rad}^L$$

Energy equation $\rightarrow$ Isothermal wind.

Radiative acceleration

Continuum acceleration

$$\mathbf{g}^C_{rad}(\mathbf{r}) = \frac{1}{c} \oint \int_{\nu=0}^{\infty} \kappa_C \, I_\nu(\mathbf{r}, \breve{\mathbf{n}}) \, \breve{\mathbf{n}} \, d\omega \, d\nu$$

can be expressed as: $g^C_{rad} = \frac{\sigma_e L_*}{4\pi r^2 c}$

$$g + g^C_{rad} = -\frac{GM_*(1-\Gamma)}{r^2} \text{ con } \Gamma = \frac{\sigma_e L_*}{4\pi c GM_*}$$

Acceleration due to momentum transfer in spectral lines

$$\mathbf{g}^L_{rad}(\mathbf{r}) = \sum_{lineas} \frac{\kappa_L \Delta\nu_D}{c} \oint \int_{x=-\infty}^{\infty} \phi\left(x - \frac{\breve{\mathbf{n}} \cdot \mathbf{v}(\mathbf{r})}{v_{th}}\right) I_\nu(\mathbf{r}, \breve{\mathbf{n}}) \, \breve{\mathbf{n}} \, d\omega \, dx$$

Sobolev approximation

For a small resonance region

$$\mathbf{g}^L_{rad} = \sum_{lineas} \frac{\kappa_L \nu_0 v_{th}}{c^2} \oint I^c(\omega) \, \breve{\mathbf{n}} \, d\omega \left[\frac{1 - e^{-\tau_0}}{\tau_0}\right]$$

Sobolev optical depth

$$\tau_{sob} = \tau_0 \, \Phi = \kappa_L \, \rho \left(\frac{v_{th}}{\mu^2 \frac{\partial v}{\partial r} + (1-\mu^2) \frac{v}{r}}\right) \Phi$$

Parameterization of the radiation force due to the spectral lines

Castor, Abbott, & Klein (1975)

$$g_{rad}^{L} = \frac{\sigma_e F}{c} \mathscr{M}(t)$$

Force multiplier

$$\mathscr{M}(t) = \sum_{lines} \frac{\Delta\nu_D F_\nu}{F} \frac{1}{t} (1 - e^{-\eta t})$$

$$\eta = \frac{\pi e^2}{m_e c} g_u f_{ul} \frac{n_l/g_l - n_u/g_u}{\rho\, \sigma_e\, \Delta\nu_D}$$

Force multiplier (Abbott,1982)

$$\mathscr{M}(t) = k\, t^{-\alpha} \left(\frac{n_e}{W(r)}\right)^{\delta}$$

with parameters k , α y δ

Interpretation of parameters

- k $\longrightarrow$Effective number of contributing lines for momentum
- α $\longrightarrow$Slope of line intensity distribution

  $$dN(\nu, \kappa_L) = -N_0\, f_\nu(\nu)\, \kappa_L^{\alpha-2}\, d\nu\, d\kappa_L$$

  that allows us to write:

  $$\sum_{lineas} g_{rad}^{L} \rightarrow \int g_{rad}^{L} dN/d\kappa_L d\kappa_L$$
- δ $\longrightarrow$ionization structure of the wind

Line-force parameters

$T_{\rm eff}$ [K]	log g	k	α	δ	Fuente
10 000	1.5	0.36	0.54	0.05	A82
15 000	2.0	0.26	0.51	0.12	A82
20 000	2.5	0.32	0.56	0.02	P86
30 000	3.5	0.17	0.59	0.09	P86

A82: Abbott(1982) - P86: Pauldrach+(1986)

β Velocity Law

Solution of the hydrodynamic equations (CAK)

Velocity law with $\beta = 0.5$

$$v(r) = v_\infty \left(1 - b\frac{R_*}{r}\right)^\beta \text{ with } b = 1 - \left(\frac{v(R_*)}{v_\infty}\right)^{\frac{1}{\beta}}$$

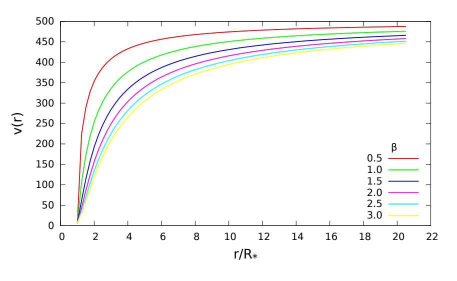

This law is commonly used with β values of 2, 3 or higher, particularly in B supergiants.

Improvements to CAK theory [modified CAK theory or m-CAK]

- Correction for finite star size.
- Inclusion of rotation.

(Pauldrach, Puls & Kudritzki, 1986; Friend & Abbott, 1986)

WLR from m-CAK theory

Wind-momentum luminosity relation (WLR)

Modified momentum rate vs luminosity

$$D_{mom} = \dot{M}\, v_{\infty} \left(\frac{R_*}{R_{\odot}}\right)^{1/2}$$

$$\log D_{mom} = x \log\left(L_* / L_{\odot}\right) + \log D_0$$

Puls+(1996) - Kudritzki+(1997)

It would enable the measurement of extragalactic distances using the stellar wind properties (D_{mom}).

WLR for OBA supergiants

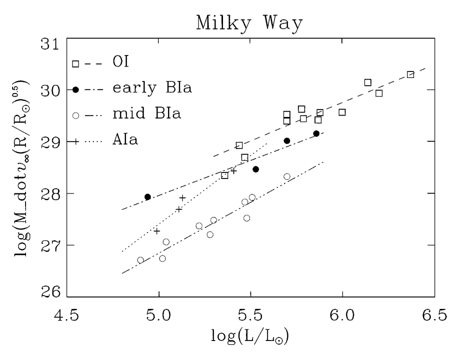

Kudritzki & Puls(2000)

Rotating radiation-driven winds

Equations for a rotating wind

1D symmetry in the equatorial plane.

Mass conservation: $F_m = 4\pi r^2 \rho v = \text{constant}$

Momentum equation: $v\dfrac{dv}{dr} = -\dfrac{1}{\rho}\dfrac{dp}{dr} - \dfrac{G\,M_*(1-\Gamma)}{r^2} + \dfrac{v_\phi^2(r)}{r} + g^L\left(\rho, \dfrac{dv}{dr}, n_e\right)$

Energy equation $\rightarrow$ Isothermal wind

Centrifugal force

$$v_\phi^2/r = v_{\rm rot}^2\, R_*^2/r^3$$

$v_{\rm rot}$ is the equatorial rotation speed

Rotational rate Ω

$$\Omega = v_{\rm rot}/v_{\rm crit} \qquad 0 \leqslant \Omega < 1$$

$$v_{\rm crit} = \sqrt{\frac{2GM_*}{3R_*}}$$

Maeder & Meynet (2000).

Hydrodynamic solutions

Fast Solution

- Classical ($\sim$m-CAK) solution
- High values of the terminal velocity
- $\Omega < 0.75$ (slow rotators)

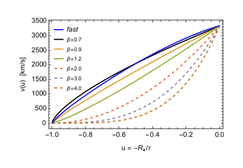

$\Omega_{\rm slow}$ solution

- Found by Curé (2004)
- $\Omega > 0.75$ (high rotators)
- Low terminal velocities and dense flows

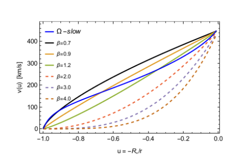

$\delta_{\rm slow}$ solution

- Found by Curé et al. (2011)
- For high values of parameter δ (changes in ionization)
- Low terminal velocities and dense flows

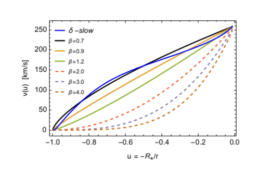

Figures from Curé & Araya (2023)
O5V star with $T_{\rm eff} = 45\,000$ K, $\log g = 4.0$, $R/R_\odot = 12$

Questions to answer

Most of B-type supergiants are not fast rotators ($\Omega \leq 0.6$)

i.e.: Howarth(2004),Hunter+(2008),Vink+(2010),de Burgos+(2023)

$\Downarrow$

We can rule out the $\Omega_{\rm slow}$ solution

We can choose between *fast* and $\delta_{\rm slow}$ solutions

Questions

- In what cases does each solution appear? Can the domains of each solution be delimited in the space of the radiation force parameters?
- Can the wind of B-type supergiants be effectively modeled using $\delta_{\rm slow}$ solutions?
- How do $\delta_{\rm slow}$ solutions modify key relations of radiation-driven wind theory such as the WLR?
- Could the transition between one solution and another explain the variability observed in the spectrum?

Calculation of wind models

Option 1

Self-consistent models

Input values

T_{eff}, log g, R_*, abundances, Ω.

Method

1) Solving hydrodynamic equations and radiation transport in moving media, including radiative acceleration calculated consistently with NLTE rates.

2) Generating the synthetic spectrum.

3) Comparison with observations.

4) Iterative refinement process.

Mostly for O-type and WR stars.

Pauldrach+(1994), Krtička & Kubát(2001, 2017), Sander+(2017), Sundqvist+(2019), Björklund+(2021), Poniatowski+(2021,2022).

Option 2

Partially consistent models

Input values

T_{eff}, log g, R_*, Ω, abundances, α , δ , k .

Method

1) Solving the hydrodynamic equations adopting a parameterization for the radiative acceleration.

2) Solving the radiation transport equation for moving media, using the hydrodynamic solution.

3) Generating the synthetic spectrum.

4) Comparison with observations.

5) Iterative refinement process.

Taresch+(1997), Pauldrach+(2001), Noebauer & Sim(2015), Lattimer & Cranmer(2021)

Option 3

Non-consistent models

Input values

T_{eff}, log g, R_*, Ω, abundances, β, $\dot{M}$, v_∞.

Method

1) Employing a β velocity law instead of solving the hydrodynamic equations.

2) Solving the radiation transport equation for moving media, using the β law.

3) Obtaining the synthetic spectrum.

4) Comparison with observations.

5) Process iteration.

Crowther+(2006), Markova & Puls(2008), Searle+(2008), Haucke+(2018)

Calculation codes

We choose option 2 because, currently, there are no self-consistent codes that produce the $\delta_{\rm slow}$ solution.

Hydrodinamic equations

HYDWIND

Curé and collaborators (Univ. Valparaíso, Chile)

Basic features

- Input: Fundamentales parameters, Ω, k , α y δ .
- Spherical Symmetry - Equatorial plane
- Inner boundary condition adopted:

$$\int_{R_*}^{\infty} \sigma_e \rho(r) dr = 2/3 \text{ or } \rho(R_*) = \rho_*$$

- Execution time: few minutes.
- It gives *fast*, $\Omega_{\rm slow}$, or $\delta_{\rm slow}$ solutions.
- Output: radial grid, velocities and densities for the wind.

Radiative transfer

FASTWIND

Puls and collaborators (LMU Munich)

Basic features

- Input: Fundamental parameters, hydro solution (or β, v_∞, $\dot{M}$).
- Spherical Symmetry.
- NLTE code considering *line blanketing*.
- Radiative transfer in Sobolev approximation and CMF.
- Unified model (photosphere + wind).
- Diagnostic range: optical.
- Execution time: 15 - 30 min.
- Output: continuum radiation distribution + line profiles (H, He, Si, C, N, O).

Most suitable δ values for B-type supergiants

Do values of δ higher than $\sim$0.25 exist in a stellar wind to achieve a $\delta_{\rm slow}$ solution?

δ values for BSGs

Early calculations indicate $\delta \lesssim 0.12$ (Abbott, 1982; Pauldrach+. 1986).

Most recent non-LTE calculations for line-force parameters assume the material to be 'frozen in ionization' ($\delta = 0$), e.g. Noebauer & Sim(2015), Lattimer & Cranmer (2021), or are limited to O-type supergiants (Gormaz-Matamala+2019,2022).

Puls, Springmann & Lennon (2000) analytically derived $\delta \gtrsim 1/3$ for a medium composed of neutral hydrogen as a trace element.

Kudritzki (2002) demonstrated that $\delta \sim 1$ for winds of low optical depth and very low metalicity.

We postulate that BSGs have a different ionization structure compared with O-type stars.

First, we examine the distribution of solution domains based on the values of the line-force parameters (k , α , δ).

Solution domains in δ and Ω space

Model T19

$T_{\rm eff} = 19$ kK

$\log g = 2.50$

$R_* = 40\ R_\odot$

S. Type: $\sim$ B2 I

$\alpha = 0.5$

$k = 0.32$

$[\,\dot{M}\,] \equiv 10^{-6}\ M_\odot\ \mathrm{yr}^{-1}$

$[\,v_\infty\,] \equiv \mathrm{km\ s}^{-1}$

Distribution of solutions

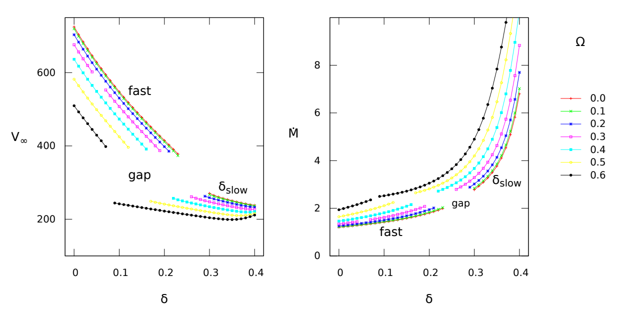

There exists a distinct **gap** between *fast* and $\delta_{\rm slow}$ solutions.

The HYDWIND code does not identify any stationary solution within the gap.

The gap is consistently present in all models, regardless of the values of $T_{\rm eff}$, $\log g$, or Ω.

Interaction between k and δ, and the wind parameters

Model T19

$\alpha = 0.5$
$\Omega = 0$

The value of v_∞ remains unchanged when different values of k are considered.

There is no change in the position or width of the gap (in δ space).

Dependence of solutions on the parameter k

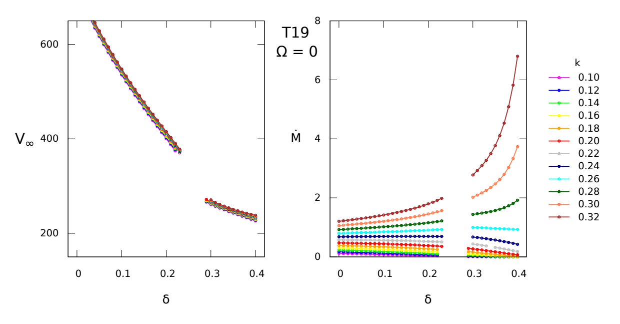

Interaction between k and δ, and the mass-loss rates

Model T19

The mass loss can either increase or decrease with δ, depending on the value of k, in both the *fast* and the $\delta_{\rm slow}$ regimes.

There is no change in the position or width of the gap (in δ space).

Dependence of solutions on the parameter k

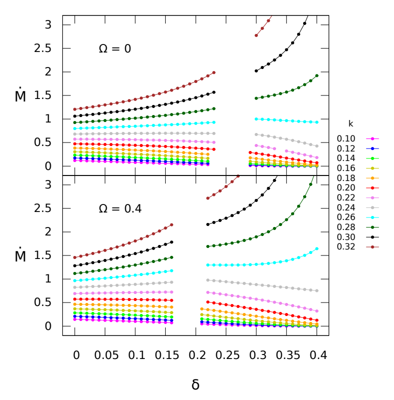

Interaction between k and δ, and the wind parameters

Model T19

The change in the slope of $\dot{M}$ as a function of $\delta_{\rm slow}$ for $k = 0.1$, 0.2, and 0.32. In contrast, the slope in v_∞ does not change.

Dependence of solutions on the parameter k

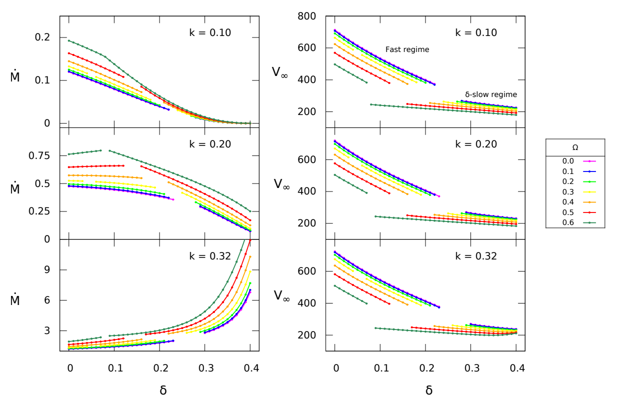

Interaction between α and δ, and the wind parameters

Model T19

In contrast to the parameter k, α completely modifies the terminal velocities.

$\dot{M}$ is also highly sensitive to this parameter.

Changing the value of α also alters the gap in δ.

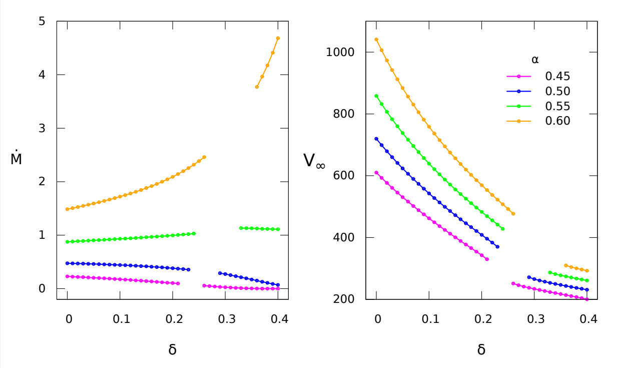

Gap Properties

Gap location

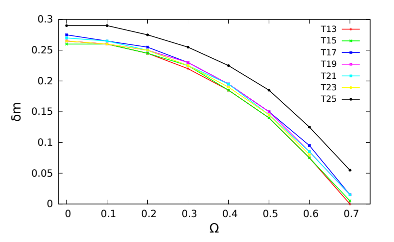

- δ_m represents the average value of δ across the edges of the gap.
- The location of the gap is almost independent of T_{eff}.
- For B supergiants exhibiting higher rotation rates, the gap is located at small values of δ.

Gap width

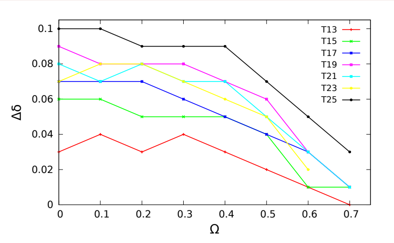

- $\Delta\delta$ is the width of the gap in δ values.
- The width decreases as Ω increases.
- Gaps are narrower in models with lower T_{eff}.

Gap Properties

Jump in v_∞

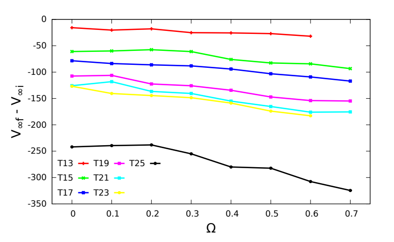

- There is little to no change in v_∞ for low T_{eff}.
- The jump increases in magnitude for faster rotators.

Jump in $\dot{M}$

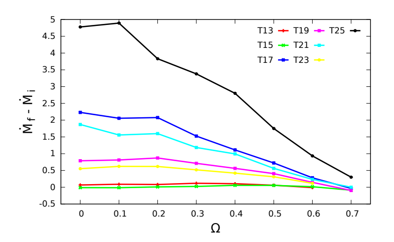

- The jump in $\dot{M}$ is smaller for larger rotators.
- $\dot{M}$ can double its value if changes in δ result in crossing the gap.

Line profiles from different wind regimes

Hα line profiles

Comparison of line profiles from *fast* and $\delta_{\rm slow}$ models with those from the β velocity law.

The models have nearly identical values of Q.

The Hα profiles generated by the *fast* and $\delta_{\rm slow}$ regimes are quite similar.

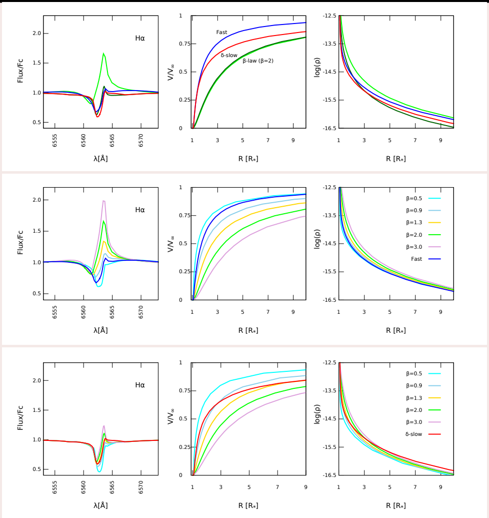

Hα line profiles

Hα line profiles for different wind regimes (model T19)

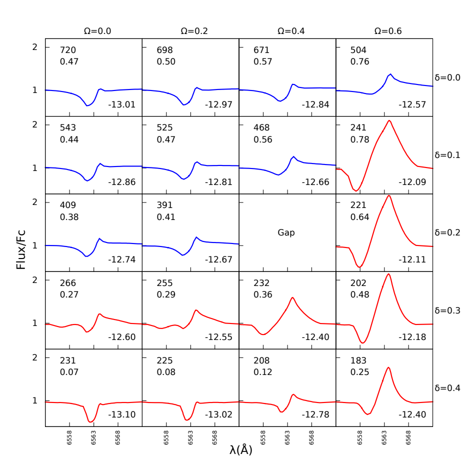

Dependence of Hα on Ω and δ

Sample of Hα line profiles for model T19.

Terminal velocities and mass-loss rates [in units of $10^{-6} M_{\odot}$ yr^{-1}]. The values of log Q are at bottom right.

Hα line profiles

Hα line dependence on the parameter k

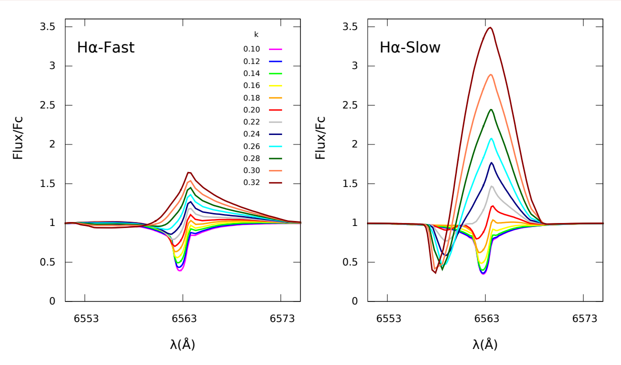

Hα line profiles

Hα line dependence on the parameter α

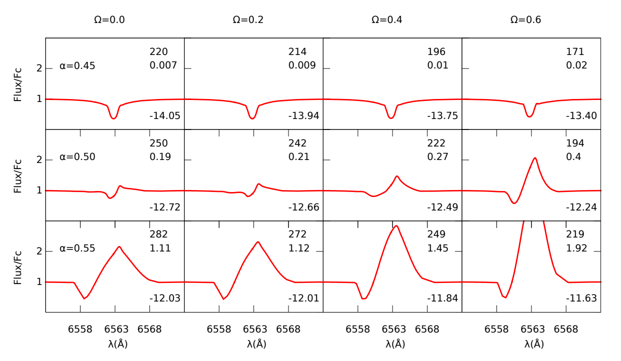

Comparison with observations

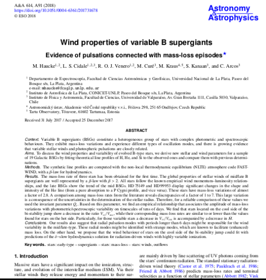

A&A 614, A91 (2018)
https://doi.org/10.1051/0004-6361/201731678

Astronomy & Astrophysics

Wind properties of variable B supergiants

Evidence of pulsations connected with mass-loss episodes★

M. Haucke[1,2], L. S. Cidale[1,2,3], R. O. J. Venero[1,2], M. Curé[3], M. Kraus[4,5], S. Kanaan[3], and C. Arcos[3]

[1] Departamento de Espectroscopía, Facultad de Ciencias Astronómicas y Geofísicas, Universidad Nacional de La Plata, Paseo del Bosque s/n, La Plata, Argentina
e-mail: mhaucke@fcaglp.unlp.edu.ar
[2] Instituto de Astrofísica de La Plata, CONICET-UNLP, Paseo del Bosque s/n, La Plata, Argentina
[3] Instituto de Física y Astronomía, Facultad de Ciencias, Universidad de Valparaíso, Av. Gran Bretaña 1111, Casilla 5030, Valparaíso, Chile
[4] Astronomický ústav, Akademie věd České republiky v.v.i., Fričova 298, 251 65 Ondřejov, Czech Republic
[5] Tartu Observatory, Tõravere, 61602 Tartumaa, Estonia

Received 31 July 2017 / Accepted 25 December 2017

ABSTRACT

Context. Variable B supergiants (BSGs) constitute a heterogeneous group of stars with complex photometric and spectroscopic behaviours. They exhibit mass-loss variations and experience different types of oscillation modes, and there is growing evidence that variable stellar winds and photospheric pulsations are closely related.
Aims. To discuss the wind properties and variability of evolved B-type stars, we derive new stellar and wind parameters for a sample of 19 Galactic BSGs by fitting theoretical line profiles of H, He, and Si to the observed ones and compare them with previous determinations.
Methods. The synthetic line profiles are computed with the non-local thermodynamic equilibrium (NLTE) atmosphere code FASTWIND, with a β-law for hydrodynamics.
Results. The mass-loss rate of three stars has been obtained for the first time. The global properties of stellar winds of mid/late B supergiants are well represented by a β-law with $\beta > 2$. All stars follow the known empirical wind momentum-luminosity relationships, and the late BSGs show the trend of the mid BSGs. HD 75149 and HD99953 display significant changes in the shape and intensity of the Hα line (from a pure absorption to a P Cygni profile, and vice versa). These stars have mass-loss variations of almost a factor of 2.8. A comparison among mass-loss rates from the literature reveals discrepancies of a factor of 1 to 7. This large variation is a consequence of the uncertainties in the determination of the stellar radius. Therefore, for a reliable comparison of these values we used the invariant parameter Q_r. Based on this parameter, we find an empirical relationship that associates the amplitude of mass-loss variations with photometric/spectroscopic variability on timescales of tens of days. We find that stars located on the cool side of the bi-stability jump show a decrease in the ratio V_∞/V_{esc}, while their corresponding mass-loss rates are similar to or lower than the values found for stars on the hot side. Particularly, for those variable stars a decrease in V_∞/V_{esc} is accompanied by a decrease in $\dot{M}$.
Conclusions. Our results also suggest that radial pulsation modes with periods longer than 6 days might be responsible for the wind variability in the mid/late-type. These radial modes might be identified with strange modes, which are known to facilitate (enhanced) mass loss. On the other hand, we propose that the wind behaviour of stars on the cool side of the bi-stability jump could fit with predictions of the δ-slow hydrodynamics solution for radiation-driven winds with highly variable ionization.

Key words. stars: early-type – supergiants – stars: mass-loss – stars: winds, outflows

1. Introduction

Massive stars have a significant impact on the ionization, structure, and evolution of the interstellar medium (ISM). Via their stellar winds they release energy and momentum to their sur-

are mainly driven by line scattering of UV photons coming from the stars' continuum radiation. The standard stationary radiation-driven wind theory (Castor et al. 1975; Pauldrach et al. 1986; Friend & Abbott 1986) predicts mass-loss rates and terminal velocities as a function of stellar parameters (Abbott 1982; Vink

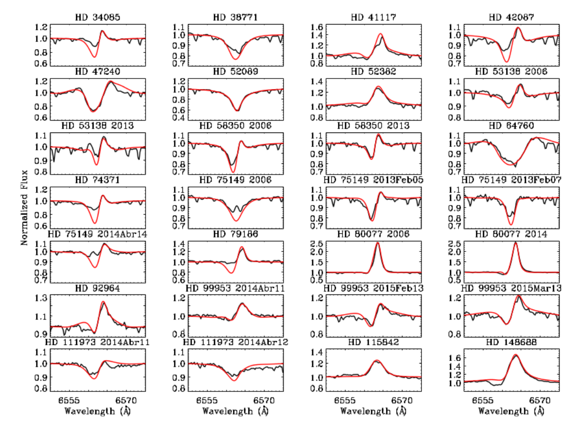

Comparison with observations

Star	Spectral type	$T_{\rm eff}$ (kK)	log g (dex)	R_* ($R_\odot$)	log $L/L_\odot$ (dex)	$v \sin i$ (km s^{-1})	$v_{\rm rot}$ (km s^{-1})	$v_{\rm mic}$ (km s^{-1})	$v_{\rm mac}$ (km s^{-1})
HD 47 240	B1 Ib	19.0	2.40	30	5.02	95	122	10	60
HD 99 953	B1/2 Iab/b	19.0	2.30	25	4.87	50	64	18	50
HD 41 117	B2 Ia	19.0	2.30	23	4.79	40	51	10	65
HD 80 077	B2 Ia + e	17.7	2.20	195	6.53	10	13	10	10*
HD 92 964	B2.5 Ia	18.0	2.20	70	5.67	45	58	11	40
HD 53 138	B3 Ia	18.0	2.25	46	5.30	40	51	10	80*
HD 75 149	B3 Ia	16.0	2.10	61	5.34	40	51	11	52
HD 42 087	B4 Ia	16.5	2.45	55	5.31	80	103	15	80
HD 58 350	B5 Ia	15.0	2.00	54	5.12	40	51	12	70
HD 79 186	B5 Ia	15.8	2.00	61	5.32	40	51	11	53
HD 74 371	B6 Iab/b	13.7	1.80	73	5.23	30	39	10	60
HD 34 085	B8 Iae	12.7	1.70	72	5.08	30	39	10	52

Stellar parameters (Haucke+2018)

Comparison with observations

Hα line profiles

Observations were performed at CASLEO using the REOSC spectrograph (2005-2015).

A subsample of stars was selected based on the presence of emission in the Hα line profile.

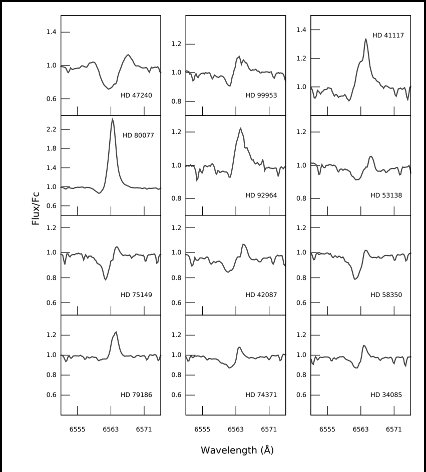

Comparison with observations

Hα line profiles

Fast regime fittings

When fitting the line profiles, we primarily focus on adjusting the emission component of the P Cygni profile.

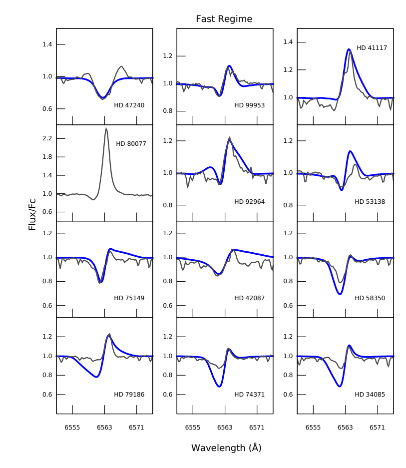

Comparison with observations

Hα line profiles

$\delta_{\rm slow}$ regime fittings

The wings appear slightly improved compared to the *fast* case.

However, many absorption components are still too deep.

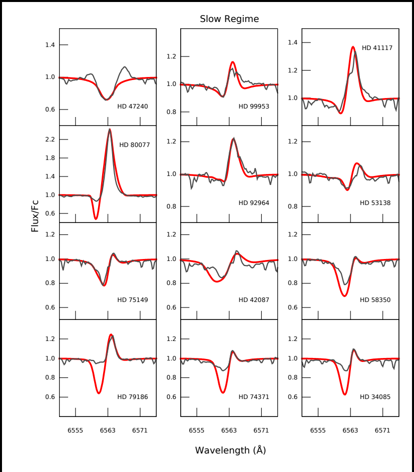

Comparison with observations

Hα line profiles

There are no significant differences between the Hα fittings for both the *fast* and δ_{slow} regimes.

Hα dichotomy

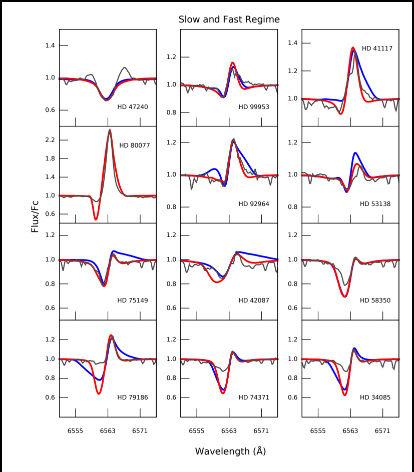

Wind parameters from fittings

Fast regime

Star	Ω	v_{crit}	v_∞	$\dot{M}$	k	α	δ	log D_{mom}
HD 47240	0.55	222.5	347.2	0.075	0.070	0.500	0.000	26.96
HD 99953	0.33	191.7	193.8	0.080	0.090	0.494	0.150	26.69
HD 41117	0.27	183.9	306.9	0.179	0.113	0.520	0.000	27.22
HD 80077	0.03	470.0	–	–	–	–	–	–
HD 92964	0.20	287.1	317.5	0.640	0.120	0.500	0.200	28.03
HD 53138	0.21	238.8	227.5	0.205	0.190	0.420	0.170	27.30
HD 75149	0.23	224.8	450.1	0.443	0.155	0.480	0.000	27.99
HD 42087	0.35	290.7	622.8	0.826	0.530	0.420	0.000	28.38
HD 58350	0.27	187.5	179.0	0.184	0.240	0.420	0.170	27.18
HD 79186	0.24	209.2	399.1	0.714	0.140	0.510	0.000	28.15
HD 74371	0.22	176.8	211.9	0.323	0.190	0.450	0.120	27.57
HD 34085	0.25	154.0	256.3	0.339	0.150	0.500	0.050	27.67

δ_{slow} regime

Star	Ω	v_{crit}	v_∞	$\dot{M}$	k	α	δ	log D_{mom}	v_∞^{Ha18}	$\dot{M}^{Ha18}$	β^{Ha18}	log D_{mom}^{Ha18}
HD 47240	0.55	222.5	161.3	0.020	0.090	0.500	0.300	26.04	450	0.24	1	27.57
HD 99953	0.33	191.7	152.5	0.061	0.080	0.530	0.320	26.47	500	0.13	2	27.33
HD 41117	0.27	183.9	160.0	0.089	0.095	0.510	0.240	26.63	510	0.17	2	27.38
HD 80077	0.03	470.0	211.0	6.379	0.606	0.300	0.295	29.07	200	5.4	3.2	28.86
HD 92964	0.20	287.1	207.0	0.363	0.130	0.505	0.350	27.60	370	0.49	2	27.98
HD 53138	0.21	238.8	211.2	0.149	0.090	0.550	0.320	27.13	600	0.24	2	27.79
HD 75149	0.23	224.8	181.6	0.171	0.185	0.480	0.310	27.18	350	0.2	2.5	27.54
HD 42087	0.35	290.7	230.4	0.354	0.452	0.480	0.405	27.58	700	0.57	2	28.27
HD 58350	0.27	187.5	182.5	0.181	0.120	0.550	0.290	27.18	233	0.15	3	27.21
HD 79186	0.24	209.2	185.3	0.381	0.110	0.550	0.300	27.54	400	0.4	3.3	27.90
HD 74371	0.22	176.8	157.6	0.247	0.163	0.501	0.270	27.32	155	0.23	2.6	27.22
HD 34085	0.25	154.0	138.5	0.176	0.180	0.500	0.280	27.11	155	0.23	2.6	27.22

Comparison with values from previous works

Comparison of terminal velocities and mass loss rates as a function of effective temperature.

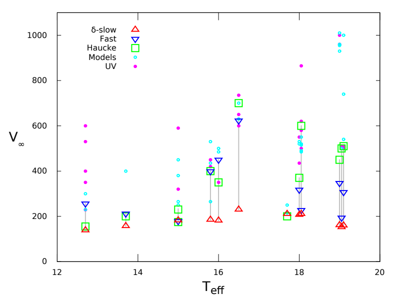

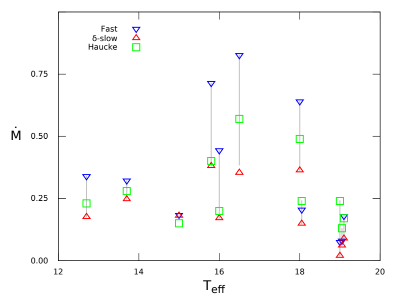

Models & UV points were taken from literature.

- Generally, the δ_{slow} solution yields the lowest values for the wind parameters.
- The *fast* solution provides values greater than those predicted by the β law.
- The measured values of v_∞ (UV) exceed those obtained by all models.

Solution domains in δ and Ω space

Model T19

$T_{\rm eff} = 19$ kK

$\log g = 2.50$

$R_* = 40\ R_\odot$

S. Type: $\sim$ B2 I

$\alpha = 0.5$

$k = 0.32$

$[\dot{M}] \equiv 10^{-6}\ M_\odot\ {\rm yr}^{-1}$

$[v_\infty] \equiv {\rm km\ s}^{-1}$

Distribution of solutions

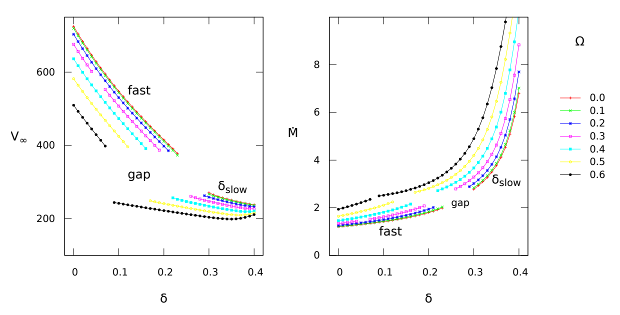

There exists a distinct **gap** between *fast* and $\delta_{\rm slow}$ solutions.

The HYDWIND code does not identify any stationary solution within the gap.

The gap is consistently present in all models, regardless of the values of $T_{\rm eff}$, $\log g$, or Ω.

Discussion

Wind momentum - Luminosity relation

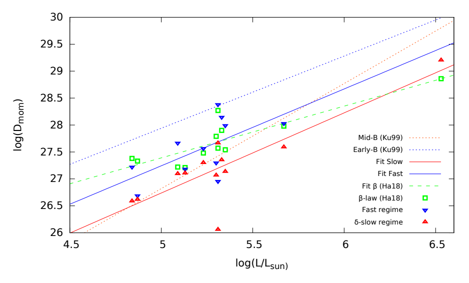

- The WLR based on the δ_{slow} solution models is close to the empirical behaviour of the mid-B supergiants (Kudritzki+,1999).
- The WLR based on the *fast* solution is in better agreement with the results from Haucke+(2018) using a β-law.
- Both relations show a considerable dispersion.

Linear regressions

δ_{slow} regime

$$\log\ D_{\text{mom}} = 1{,}48\ \log\ L/L_{\odot} + 19{,}30$$

fast regime

$$\log\ D_{\text{mom}} = 1{,}43\ \log\ L/L_{\odot} + 20{,}11$$

Discussion

The gap and the variability

- A change in wind regime can occur as a result of variations in δ.
- A higher rotational rate Ω reduces the required change in δ to transition between regimes.
- Could these changes in regime be due to binaries or stellar pulsations?

Jumping the gap

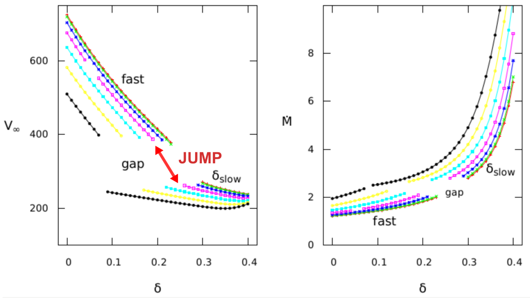

Conclusions

Hydrodynamic solutions

- We determined the domains of hydrodynamic solutions. The *fast* and $\delta_{\rm slow}$ regimes are separated by a gap where no stationary solutions were found using the available codes.
- This distribution of domains is consistent across spectral subtypes.
- Rotation affects the distribution of domains.

Line profiles

- For the first time, we have fitted synthetic line profiles computed with the hydrodynamic solution $\delta_{\rm slow}$ to observed ones for B supergiant stars.
- Hα line profiles can be fitted with both *fast* and $\delta_{\rm slow}$ models.
- The $\delta_{\rm slow}$ solution could be suitable for modeling the winds of certain B supergiants.
- Our fits predict a WLR close to that found for intermediate B supergiants.
- However, this solution is constrained by the maximum terminal velocity the wind can achieve. Consequently, it cannot account for the measured (or estimated) v_∞ values in the UV for B supergiants.

Future work

- Given that Hα may not be the most suitable line for determining the most appropriate wind regime, this analysis should be expanded to include other spectral ranges, particularly IR and UV.
- This study analyzed only 12 stars. To reach a definitive conclusion, a larger sample is needed.
- Since the only hypergiant B in the sample was fitted exclusively with the $\delta_{\rm slow}$ solution, further testing on a larger sample of hypergiants B would be intriguing. Moreover, some published works suggest employing a double-β velocity law, which closely resembles the $\delta_{\rm slow}$ solution.
- The variability observed in the spectra of these stars could be explained by certain scenarios involving alternations in hydrodynamic solutions.


Спасибо!
Děkuji!
¡GRACIAS!
Aitäh!
Danke!
Obrigado!
Thank you!
Təşəkkürlər!

The End


GRACIAS

Discussion

Escenario

- Una mancha caliente en la superficie de una SG con viento dominado por la solución rápida.
- Su alta ionización origina una región con viento dominado por la solución δ_{slow} (lento y denso).
- Cambios de régimen secuenciales en el período rotacional.
- Posible origen de (DACs).

Modelo CIR

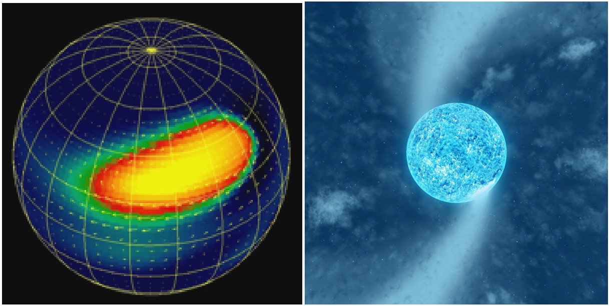

Una curiosidad

Zeta Puppis (O4) y otras supergigantes tienen bright spot

MNRAS **000**, 1–40 (2017) Preprint 25 October 2017 Compiled using MNRAS LaTeX style file v3.0

BRITE-Constellation high-precision time-dependent photometry of the early-O-type supergiant ζ Puppis unveils the photospheric drivers of its small- and large-scale wind structures

Tahina Ramiaramanantsoa,[1,2*] Anthony F. J. Moffat,[1,2] Robert Harmon,[3] Richard Ignace,[4] Nicole St-Louis,[1,2] Dany Vanbeveren,[5] Tomer Shenar,[6] Herbert Pablo,[1,2] Noel D. Richardson,[7] Ian D. Howarth,[8] Ian R. Stevens,[9] Caroline Piaulet,[1] Lucas St-Jean,[1] Thomas Eversberg,[10] Andrzej Pigulski,[11] Adam Popowicz,[12] Rainer Kuschnig,[13] Elżbieta Zocłońska,[14] Bram Buysschaert,[15,16] Gerald Handler,[14] Werner W. Weiss,[13] Gregg A. Wade,[17] Slavek M. Rucinski,[18] Konstanze Zwintz,[19] Paul Luckas,[20] Bernard Heathcote,[21] Paulo Cacella,[22] Jonathan Powles,[23] Malcolm Locke,[24] Terry Bohlsen,[25] André-Nicolas Chené,[26] Brent Miszalski,[27,28] Wayne L. Waldron,[29] Marissa M. Kotze,[27,28] Enrico J. Kotze[27] and Torsten Böhm[30,31]

Affiliations are listed at the end of the paper

Accepted 2017 October 11. Received 2017 September 22; in original form 2017 May 23

ABSTRACT

From 5.5 months of dual-band optical photometric monitoring at the 1 mmag level, *BRITE-Constellation* has revealed two simultaneous types of variability in the O4I(n)fp star ζ Puppis: one single periodic non-sinusoidal component superimposed on a stochastic component. The monoperiodic component is the 1.78 d signal previously detected by *Coriolis*/SMEI, but this time along with a prominent first harmonic. The shape of this signal changes over time, a behaviour that is incompatible with stellar oscillations but consistent with rotational modulation arising from evolving bright surface inhomogeneities. By means of a constrained non-linear light curve inversion algorithm we mapped the locations of the bright surface spots and traced their evolution. Our simultaneous ground-based multi-site spectroscopic monitoring of the star unveiled cyclical modulation of its He II λ4686 wind emission line with the 1.78-day rotation period, showing signatures of Corotating Interaction Regions (CIRs) that turn out to be driven by the bright photospheric spots observed by *BRITE*. Traces of wind clumps are also observed in the He II λ4686 line and are correlated with the amplitudes of the stochastic component of the light variations probed by *BRITE* at the photosphere, suggesting that the *BRITE* observations additionally unveiled the photospheric drivers of wind clumps in ζ Pup and that the clumping phenomenon starts at the very base of the wind. The origins of both the bright surface inhomogeneities and the stochastic light variations remain unknown, but a subsurface convective zone might play an important role in the generation of these two types of photospheric variability.

Key words: stars: massive — stars: rotation: starspots — stars: winds, outflows — technique: photometry — technique: spectroscopy

* E-mail: tahina@astro.umontreal.ca